

| | |
|---------------|---|
| k_3, k_{-3} | pseudo-first-order rate constants for isomerization of the 1,2-polybutadiene hydroformylated product appearing in eqs 3 and 4, s^{-1} |
| k_4 | pseudo-first-order rate constant for 1,4-polybutadiene hydroformylation to the internally branched aldehyde product appearing in eq 5, s^{-1} |
| k_{12} | pseudo-first-order rate constant for hydroformylation of pure 1,2-polybutadiene appearing in eq 7, s^{-1} |
| k_{14} | pseudo-first-order rate constant for hydroformylation of pure 1,4-polybutadiene appearing in eq 6, s^{-1} |
| R_{12} | reaction rate for hydroformylation of 1,2-polybutadiene defined by eq 7, mol/(L min) |
| R_{14} | reaction rate for hydroformylation of 1,4-polybutadiene defined by eq 6, mol/(L min) |
| t | reaction time, s |

Subscripts

| | |
|-----|--|
| 12 | denotes 1,2-butadiene or 1,2-polybutadiene |
| 14 | denotes 1,4-butadiene or 1,4-polybutadiene |
| ole | denotes the butadiene unit |

References and Notes

- (1) Cull, N. L.; Mertzweiler, J. K.; Tenney, H. M. (Esso Research and Engineering Company) U.S. Patent 3 383 426, 1968.
- (2) Ramp, F. L.; Dewitt, E. J.; Trapasso, L. E. *J. Polym. Sci.* **1966**, *4*, 2267.
- (3) Sanui, K.; MacKnight, J. W.; Lenz, R. W. *Macromolecules* **1974**, *7*, 952.
- (4) Mohammadi, N. A.; Rempel, G. L. In *Chemical Reactions on Polymers*; Benham, J. L., Kinstle, J. F., Eds.; ACS Symposium Series 364; American Chemical Society: Washington, DC, 1988; pp 373-408.
- (5) Hedrick, R. M.; Gabbert, J. D. *Reaction Injection Molding of Nylon 6 Block Copolymer*, Second World Congress of Chemical Engineering; Montreal, Canada, Oct 1981.
- (6) Hedrick, R. M.; Gabbert, J. D. Nylon Block Copolymer for a New Reaction Injection Molding System. Paper presented at the SITEV 1982 Meeting, Geneva, Switzerland, May 1982.
- (7) Gabbert, J. D.; Garner, A. Y.; Hedrick, R. M. Developments in Nylon 6 Block Copolymer RIM. Society of Automotive Engineers International Congress and Exposition, Detroit, MI, Feb 1982; SAE Technical Paper Series No. 820420.
- (8) Cornils, B. In *New Synthesis with Carbon Monoxide*; Falbe, J., Ed.; Springer-Verlag: New York, 1980.
- (9) Brown, C. K.; Wilkinson, G. *J. Chem. Soc. (A)* **1970**, 2753.
- (10) Pruett, R. L. in *Advances in Organometallic Chemistry*; Stone, F. G. A., West, R., Eds.; Academic Press: New York, 1979; Vol. 17, pp 1-60.
- (11) Balhiser, R. E.; Samuels, M. R.; Eliassen, J. D. *Chemical Engineering Thermodynamics. The Study of Energy, Entropy, and Equilibrium*; Prentice-Hall: New Jersey, 1972.
- (12) Pruett, R. L.; Smith, J. A. *J. Organomet. Chem.* **1969**, *34*, 327.
- (13) Ramachandran, P. A.; Chaudhari, R. V. *Three-Phase Catalytic Reactors*; Gordon and Breach: London, 1985.
- (14) Kuester, J. L.; Mize, J. H. *Optimization Techniques with Fortran*; McGraw-Hill: New York, 1973.
- (15) Marquardt, D. W. *Technometrics* **1970**, *12*, 591.
- (16) Sherwood, T. K.; Reid, R. F. *The Properties of Gases and Liquids*, 2nd ed.; McGraw-Hill: New York, 1968.
- (17) Mills, P. L.; Ramachandran, P. A.; Duduković, M. P. In *Reaction Engineering for Multiphase Catalyzed Systems*; AIChE Continuing Education Lecture Notes, New York, 1988; Chapter 4.

Intermediate-Angle Neutron and X-ray Scattering Functions of Poly(methyl methacrylate) Chains

Michele Vacatello,¹ Do Y. Yoon,* and Paul J. Flory²

IBM Research Division, Almaden Research Center, 650 Harry Road,
San Jose, California 95120-6099. Received August 8, 1989;
Revised Manuscript Received October 13, 1989

ABSTRACT: The molecular scattering functions of isotactic, syndiotactic, and atactic poly(methyl methacrylate) (PMMA) chains have been calculated according to the three different rotational isomeric state (RIS) models in the literature and compared with experiments. Comparison with the neutron scattering experiments on glassy (atactic) PMMA shows that only the most rigorous six-state model predicts all the features exhibited by the experimental results over the entire scattering vector q ($= (4\pi/\lambda) \sin(\theta/2)$) to ca. 0.6 \AA^{-1} . In particular, the two-state and the three-state models predict the occurrence of a second maximum in the absolute-scale Kratky plot at values of q that are considerably smaller than the experimental results. In contrast, the scattering function calculated in the framework of the six-state model shows the two maxima and the intervening minimum in the same locations of q as those in the experimental curve. The six-state RIS model also predicts the molecular scattering functions in good agreement with the available neutron scattering results on the isotactic and syndiotactic PMMA in the bulk, up to $q \approx 0.25 \text{ \AA}^{-1}$, as well as the X-ray scattering experiments on syndiotactic PMMA in solution up to $q \approx 0.7 \text{ \AA}^{-1}$. Therefore, our results show that even in the case of a complicated looking polymer like PMMA the chain conformations in the bulk amorphous state correspond very closely to the unperturbed random coils, not only for the overall chain configuration but also for local chain segments constituted by a few units.

Introduction

It is now well-known that the elastic scattering of thermal neutrons in the small and intermediate angle region

is an invaluable, unique tool to probe the overall and the local conformations of polymer molecules in a variety of environments.³ This is due to the fact that the marked difference between the coherent scattering lengths of hy-

drogen and deuterium (-0.374×10^{-14} and 0.667×10^{-14} m, respectively) results in significant coherent scattering intensities for the dispersed deuterated polymer in a hydrogenous host (or vice versa). This allows us to label some of the chains (or selected parts of them) and to determine the molecular scattering function not only in dilute solutions but also in concentrated solutions, in the bulk amorphous state, in the semi-crystalline state, in polymer blends, etc. The information contained in the molecular scattering function is particularly relevant to the conformational properties of polymers, especially when compared with calculated results based on theoretical models of the chain conformations.

At very small angles, where the coherent scattering is determined by the spatial relationships between the monomer units which are far apart along the chain, the experimental scattering patterns are very well reproduced by the Debye equation⁴ for Gaussian coils

$$P(q) = (2/\nu^2)(\nu - 1 + e^{-\nu}) \quad (1)$$

in which $q = (4\pi/\lambda) \sin(\theta/2)$, $P(q)$ is the ratio of the coherent scattered intensity at a scattering angle θ to that at $\theta = 0$, λ is the wavelength of the incident radiation, and $\nu = q^2 \langle s^2 \rangle$, $\langle s^2 \rangle$ being the mean-square radius of gyration of the polymer. Equation 1 is based on the two assumptions that (i) the mean-square distance between units k and l in the polymer chain is proportional to $t = |k - l|$ and (ii) the Fourier transform of the density distribution of the vector r_{kl} connecting the two units is Gaussian for any value of k and l .⁴ Although both assumptions have been shown to fail in real chains for t less than approximately 100 units⁵ which determine the scattering pattern at q larger than 0.03 \AA^{-1} , the observed scattering functions are usually not too far from those predicted by equation 1 up to $q = 0.1\text{--}0.2 \text{ \AA}^{-1}$.

A noticeable exception is provided by syndiotactic and atactic poly(methyl methacrylate) (PMMA), for which the absolute-scale Kratky function, $F_x(q) (= xq^2 P(q))$, x being the degree of polymerization) passes through a maximum at $q \approx 0.08 \text{ \AA}^{-1}$, instead of showing the usual leveling off at high q values.⁶⁻¹⁰ This feature was originally assumed to indicate the existence of intra- and/or intermolecular order in solution and in the bulk amorphous polymer. On the basis of a simple two-state rotational isomeric state (RIS) model of PMMA conformations, Yoon and Flory^{11,12} demonstrated that the presence of a maximum in this region of q is compatible with the unperturbed random-coil chain statistics, which exhibits the unusual tendency of short syndiotactic PMMA sequences (10–20 units) to have characteristic ratios larger than those of longer sequences due to the presence of locally arclike conformations. Owing to this peculiarity, comparison of the experimental scattering functions of PMMA with the predictions of the theoretical calculations provides a very stringent test of the theoretical models of PMMA conformations published in the recent literature.

Current interest in this area has been motivated by a number of recent developments in both the theoretical and the experimental aspects. Following the first experimental work of Kirste and co-workers,^{6,7} the neutron scattering from mixtures of deuterated and hydrogenous PMMA has been investigated further by other groups.⁸⁻¹⁰ In particular, Dettenmaier et al.⁹ extended the measurement of the molecular scattering function of atactic-PMMA (a-PMMA) up to $q \approx 0.6 \text{ \AA}^{-1}$, from the previous maximum value of $q \approx 0.2 \text{ \AA}^{-1}$. All these measurements confirm the existence of a maximum in the Kratky function at $q \approx 0.08 \text{ \AA}^{-1}$, in good agreement with the predic-

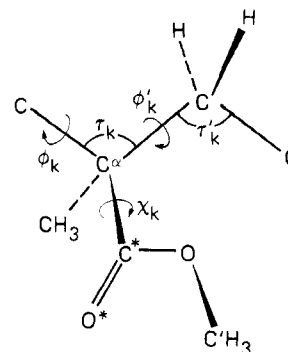


Figure 1. Schematic of the PMMA segment and the notations.

tions of the two-state RIS model of Sundararajan and Flory.¹³ This maximum is followed by a minimum at $0.32\text{--}0.34 \text{ \AA}^{-1}$, however, while the model of ref 13 predicts a minimum at 0.18 \AA^{-1} ,^{11,12} indicating that this model is not good enough to describe the detailed conformation of PMMA on a local scale.

The two-state RIS model was obtained as a result of simple conformational energy calculations based on the assumption that the plane of the ester group bisects the angle of the three nearest neighboring backbone atoms. This leads one to dismiss the \bar{g} state, owing to high repulsive interactions between the ester group and an adjacent ester or methyl group in this conformation.¹³ Experimental data from various sources indicate, on the other hand, a greater diversity of orientations of the ester groups with respect to the backbone and the necessity of including additional gauche states for the skeletal bonds.¹⁴⁻¹⁶

A more detailed examination of the conformational properties of PMMA has been recently carried out by Sundararajan¹⁷ and by Vacatello and Flory.¹⁸ In both studies the ester groups were allowed to rotate around the bonds connecting them to the backbone. Furthermore, in the work of ref 18 all the bond angles have been independently optimized in each backbone/ester group conformation. Two new RIS models, both including the \bar{g} state, have therefore been proposed as a result of these recent investigations. In view of the high sensitivity of the molecular scattering function to the details of the local chain conformations, we examine in this paper the molecular scattering functions of PMMA chains calculated according to the various models and compare them with the experimental data presently available.

Notation and Methods

PMMA is a disubstituted vinyl polymer with two different side groups, which make the skeletal bonds intrinsically chiral.¹⁹ Figures 1 and 2 show the notation adopted in this paper, following ref 19, to label the atoms, to distinguish the bond chiralities, and to name rotational states. With this notation, the isotactic polymer (i-PMMA) is described by the sequence $\cdots |dl|dl|dl| \cdots$ or $\cdots |ld|ld|ld| \cdots$, while the syndiotactic polymer (s-PMMA) is described by $\cdots |dd|ll|dd| \cdots$ or $\cdots |ll|dd|ll| \cdots$, the vertical bars representing the position of the C^α atoms. Intervals in which C^α is syn to CH_3 and CH_2 are denoted by g , while intervals in which C^α is syn to $COOCH_3$ and CH_2 are denoted by \bar{g} . Subscripts indicate the signs of departure from perfect staggering. Torsion angles around d bonds are measured in the right-hand sense, while the left-hand sense is used for l bonds in such a way that enantiomeric conformations carry identical designations. The torsion angle χ_k of Figure 1, referred to the sequence $CH_3-C^\alpha-C^*-O^*$,

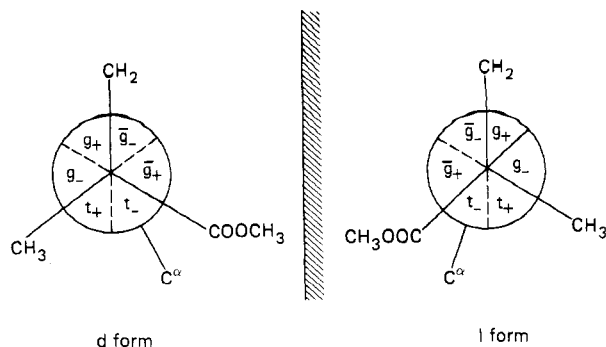


Figure 2. Conformations for enantiomeric *d* and *l* skeletal bonds of PMMA and their classification in six domains.

is measured in the reference frame of the subsequent interdiad backbone bond.

The molecular scattering function in the absolute-scale Kratky plot, $F_x(q)$, is given by¹²

$$F_x(q) = xq^2P(q) = \sum_{k,l} f_k f_l \left[\frac{q^2 \sin(qr_{0;kl})}{qr_{0;kl}} + 2q^2(x+1)^{-1} \sum_{t=1}^x (x+1-t) \left\langle \frac{\sin(qr_{t;kl})}{qr_{t;kl}} \right\rangle \right] / \sum_{k,l} f_k f_l \quad (2)$$

where $x+1$ is the number of monomer units in the polymer, $r_{t;kl}$ denotes the distance of scattering center k of a given unit to the scattering center l of the t th subsequent unit, and f_k and f_l are the scattering powers of the two centers. For x and T large enough, eq 2 can be rewritten as

$$F_x(q) = F_{0,T}(q) + F_{T+1,x}(q) = F_{0,T}(q) + 2q^2(x+1)^{-1} \sum_{t=T+1}^x (x+1-t) \left\langle \frac{\sin(qr_t)}{qr_t} \right\rangle \quad (3)$$

where $F_{0,T}(q)$ represents the contribution to $F_x(q)$ of scattering centers belonging to monomer units separated by less than T intervening units and $F_{T+1,x}(q)$ gives the contribution to $F_x(q)$ of units separated by T monomer units at least, r_t being the spatial distance of the centers of two such units. In the assumption that the distribution of r_t is Gaussian for T large, $\langle \sin(qr_t)/qr_t \rangle = \exp(-q^2 \langle r_t^2 \rangle / 6) = \exp(-\nu t / x)$. Hence, for x and T large

$$F_{T+1,x}(q) = (2x/\nu^2)q^2(e^{-\nu} - e^{-\nu T/x}(\nu T/x - \nu + 1)) \quad (4)$$

As expected, $F_{T+1,x}(q)$ is 0 when $T = x$ and $F_{T+1,x}(q)/xq^2$ coincides with $\bar{P}(q)$ given by the Debye equation when $T = 0$.

For each RIS model, $F_{0,T}(q)$ has been calculated as the average over 10 000 conformations of a chain sequence containing $T = 500$ monomer units obtained at random according to conditional probabilities as dictated by the model (see later). Scattering centers have been placed in the centers of mass of the hydrogen atoms of the CH_2 backbone groups (with $f_{\text{CH}_2} = 2$) and of the side-chain CH_3 and $\text{C}^{\alpha}\text{H}_3$ groups (with $f_{\text{CH}_3} = f_{\text{C}^{\alpha}\text{H}_3} = 3$). The contribution $F_{T+1,x}(q)$ from units between $T+1 = 501$ and $x = 1000$, which is of the order of the chain length of the polymers actually used in neutron scattering experiments, has been added by using eq 4 with the characteristic ratios 7.3, 8.5, and 10.3 for s-PMMA, a-PMMA, and i-PMMA, respectively; $F_{T+1,x}(q)$ is generally very small for this value of T and vanishes practically for $q > 0.03 \text{ \AA}^{-1}$. In the case of the six-state model, calculations have been also performed with $T = 80$ and $T = 180$. The resulting scattering functions are practically indistinguishable

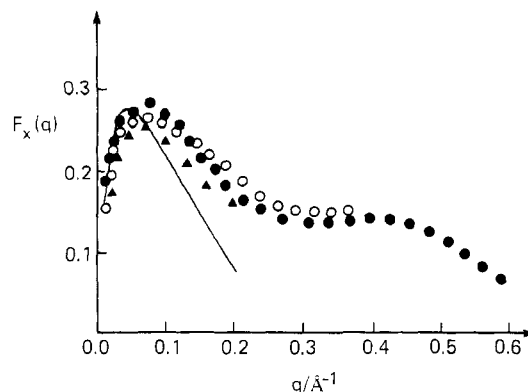


Figure 3. The molecular scattering function $F_x(q)$ (in the absolute-scale Kratky plot) of a-PMMA in the glassy state from various neutron scattering experiments: ref 7, solid line; ref 8,²⁰ triangles; ref 9, full circles; ref 10, open circles.

in the whole range of q , indicating that the two assumptions discussed in the Introduction are valid for PMMA when $t > 80$.

Calculations of $F_x(q)$ have been performed for stereochemically regular i-PMMA and s-PMMA and for polymer chains containing 10% and 20% of meso diads, respectively, since the syndiotactic polymer used in the neutron scattering experiments contains approximately 10% of meso diads, while the usual atactic PMMA is a mostly syndiotactic polymer with about 20% of meso diads.^{8,9} In the case of the syndiotactic polymer, two additional calculations have also been performed with the scattering centers placed on the backbone C^{α} carbon atoms and at the centers of mass of the ester groups, respectively (see below).

Comparison with Neutron Scattering Experiments

Figure 3 compares the molecular scattering function originally determined by Kirste et al.^{6,7} for a-PMMA in the glassy state (continuous curve) with more recent data from various sources. The triangles refer to the work of O'Reilly et al.^{8,20} The full circles show the scattering function determined by Dettenmaier et al.⁹ up to $q \approx 0.6 \text{ \AA}^{-1}$, while the open circles refer to the recent work of Ito et al.¹⁰ The unusual behavior first evidenced in refs 6 and 7 is confirmed by the more recent experiments, with the first maximum located at the scattering vector q approximately 0.08 \AA^{-1} . This maximum is followed by a minimum at $0.32\text{--}0.34 \text{ \AA}^{-1}$ and by the second maximum at $0.41\text{--}0.42 \text{ \AA}^{-1}$.

The Two-State Model. The first RIS model of the conformation of PMMA was proposed by Sundararajan and Flory¹³ in 1974 as a result of conformational energy calculations on a simplified model of a meso (*dl*) and a racemic (*dd*) diad. Hydrogen atoms of the CH_3 and CH_2 groups were not included explicitly, these groups being treated as a single atom with suitable nonbonded interaction parameters. The plane of the ester group was fixed so as to bisect the skeletal bond angle at the adjoining C^{α} atom.

A plot of the energy versus the backbone bond angle at the CH_2 group for the *tt* and the *tg* conformations of the meso diad (the torsion angles being at their staggered values 0° and 120°) revealed a minimum between 122° and 126° . With this angle fixed at 122° , energy maps were calculated for meso and racemic diads with the torsion angles χ_1 and χ_2 (see Figure 1) assigned to 0° or 180° .

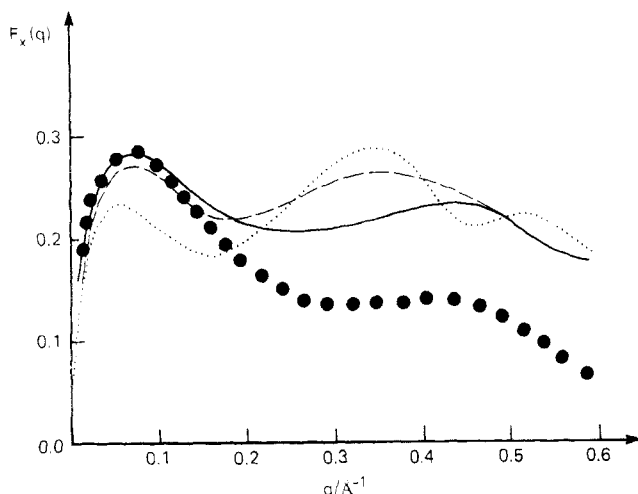


Figure 4. Comparison of the molecular scattering functions $F_x(q)$ of a-PMMA calculated according to the three models with the experimental results (filled circles) of ref 9: two-state model, dotted line; three-state model, dashed line; six-state model, solid line.

All the energy maps show minima in the tt, tg, gt, and gg domains while the energies of the states involving \bar{g} conformations are always exceedingly high. With the single exception of the racemic tt conformation, two distinct minima are present in each domain, shifted approximately $\pm 15^\circ$ with respect to perfect staggering. Successive displacements inside a diad are of opposite sign for meso diads and of the same sign for racemic diads, corresponding in both cases to displacements of the same absolute sense.

Owing to the nearly 2-fold symmetry inside each low energy domain of the energy maps, it was considered reasonable to approximate the conformational characteristics of PMMA by a two-state RIS model with the torsional angles at 0° and 120° , respectively. Statistical weight matrices were then derived according to the general treatment of ref 19, with the various parameters assessed according to the energy maps. Calculations of conformation-dependent quantities such as the characteristic ratios C_∞ and the temperature coefficients dC_∞/dT using this set of parameters led to results far from the experimental values, however. In recognition of the limited accuracy of the conformational energies, the statistical weights were then appropriately modified.

The molecular scattering function of a-PMMA calculated on the basis of this two-state model, denoted by the dotted line in Figure 4, shows three maxima at approximately $q = 0.06, 0.35$, and 0.52 \AA^{-1} , separated by minima at 0.18 and 0.46 \AA^{-1} . The position of the first maximum is not too far from that in the experimental curve. The model fails to reproduce the features of the experimental curve for $q > 0.15 \text{ \AA}^{-1}$, however. This shows that the two-state model does not correctly describe the conformational statistics of a-PMMA (and s-PMMA) on a local scale.

The Three-State Model. A three-state RIS model has been recently proposed by Sundararajan¹⁷ on the basis of calculations performed on PMMA diads using a slightly modified set of parameters (with the hydrogen atoms of the central CH_2 group explicitly included) and a different method. For each conformation of the backbone, the torsion angles χ_1 and χ_2 have been varied in steps of 10° from -40° to 40° and from 140° to 220° , while the skeletal bond angle τ has been varied in steps of 2° from 118° to 126° . Energy maps for the meso and race-

mic diads have been calculated as a function of the torsional angles ϕ'_1 and ϕ'_2 (see Figure 1), the energy in each point of the maps being the minimum value found for that backbone conformation when all the other parameters were varied.

In contrast to the results obtained in ref 13 with χ_1 and χ_2 fixed at 0° or 180° , the conformations including the \bar{g} state are found to occur with relatively low energies. Furthermore, the nearly 2-fold local symmetry of the various domains with respect to staggered positions that characterized the energy maps of ref 13 is virtually absent. As a result, a three-state RIS model is proposed in which the exact location of the states, nominally identified as t, g, and \bar{g} , depends on the torsional state of the adjacent backbone bond in the same diad. For instance, ϕ'_k of the trans state assumes the values $10^\circ, 0^\circ$, and -5° in tt, tg, and t \bar{g} of the meso diad, respectively. The exact torsional angle of a given rotational isomeric state with the same nominal designation also changes with the diad character (meso or racemic).

The results of the energy calculations have been used to establish the value of the various parameters appearing in the statistical weight matrices appropriate for a three-state RIS model of PMMA. However, characteristic ratios calculated with these values of the statistical weight parameters and with the torsional angles indicated by the energy maps are not in good agreement with the experimental results for both i-PMMA and s-PMMA. A better overall agreement with experiments is obtained when the energy parameters are adjusted, by ca. 0.5 kcal/mol , with respect to the results of the conformational energy calculations.

The molecular scattering function evaluated for a-PMMA according to the three-state model using the set of parameters (geometries, torsional angles, and energies) recommended in ref 17 (Figure 4, dashed line) shows a maximum at $q = 0.08 \text{ \AA}^{-1}$, followed by a minimum at $q = 0.18 \text{ \AA}^{-1}$ and by a second maximum at $q = 0.35 \text{ \AA}^{-1}$. (We have used the set of parameters, including the $(10^\circ, -15^\circ)$ for the meso,tt state, that yielded the best agreement with experimental results in ref 17.) The overall agreement of the calculated scattering function with the experimental curve is much better for the three-state model than for the two-state model. The position of the minimum and of the second maximum are displaced to lower values of q , however, with respect to the experimental curve. This shows that the picture of the local conformation of a-PMMA provided by the three state model still needs improvement.

The Six-State Model. Simultaneously with the development of the three-state model, a more detailed reinvestigation of the conformational properties of PMMA has been performed by Vacatello and Flory.¹⁸ All the atoms were explicitly represented, including the hydrogens of CH_3 and OC'H_3 groups. Calculations of the conformational energy were performed for short-chain model compounds and for stereoregular chains with a four-bond conformational repeat. With the four backbone torsion angles assigned starting values corresponding to any one of the domains shown in Figure 2, the energy was optimized with respect to all the bond angles and all the torsion angles including those in the backbone.

The results of these calculations show that the \bar{g} state is of low energy and is always associated with a displacement of the ester group of approximately 35° with respect to $\chi_k = 0^\circ$ or $\chi_k = 180^\circ$, the displacement being such that the plane of the ester group is almost perpendicular to the plane defined by the C-C* and the \bar{g} bond.

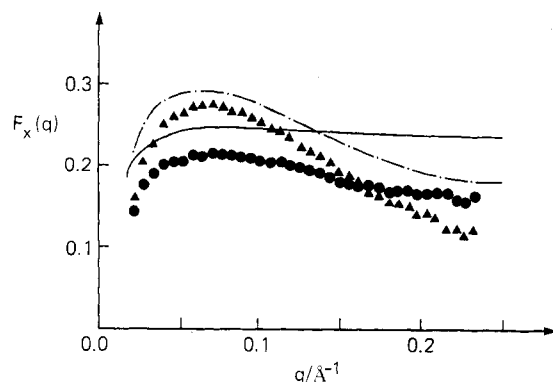


Figure 5. Comparison of the molecular scattering functions $F_x(q)$ of s-PMMA (triangles) and i-PMMA (circles) from the neutron scattering experiments of ref 8²⁰ with the corresponding curves calculated according to the six-state model: s-PMMA containing 10% meso diads, dot-dashed curve; i-PMMA, solid curve.

The intradiad bond angle τ' is almost always 124° , while the interdiad bond angle τ varies with the torsional state of the adjacent backbone bonds. It assumes the value of 106° when both bonds are in trans conformation, 111° when only one of them is in trans state, and 116° when neither is trans. The analysis of the distribution of the backbone torsion angles in chain conformations with acceptable energies shows that they can be represented according to six states located approximately at -20° (t_-), 10° (t_+), 100° (g_-), 125° (g_+), -125° (\bar{g}_-), and -100° (\bar{g}_+). The various parameters appearing in the statistical weight matrices appropriate for the six-state model of PMMA have been assessed according to the results of the energy calculations. The characteristic ratios of i-PMMA and s-PMMA and their temperature coefficients calculated by using these parameters are in excellent agreement with experiments. The same is true for the characteristic ratio of polymers with intermediate tacticity. Thus, the parameters obtained by conformational energy calculations do not require adjustments in order to reproduce these conformation-dependent quantities. This is in contrast to the situations with the two- and the three-state RIS models that required substantial adjustments of the calculated energies in order to reproduce the experimental results.

The scattering function of a-PMMA calculated according to the six-state model (Figure 4, solid line) shows two maxima separated by a minimum. The maxima are located at 0.08 and 0.41 \AA^{-1} , while the intermediate broad minimum is centered around 0.3 \AA^{-1} , in good agreement with experiments. More detailed calculations that take into account the actual position of each deuterium show little difference from the curve in Figure 4.

The results of Figure 4 show that the absolute intensities of the calculated curves are always higher than the experimental results for values of $q > 0.2 \text{ \AA}^{-1}$. At present, there is no simple explanation for this discrepancy. Since the average absolute intensity of the calculated curves is almost the same in this q region for the three models, which are sufficiently different in the position and relative frequency of the conformational states, the discrepancy seems most likely to be related to the subtraction of the incoherent scattering contribution, which is very sensitive to small errors at high values of q . For example, ca. 2% error in the incoherent scattering at $q = 0.1 \text{ \AA}^{-1}$ would result in ca. 50% error in the $F_x(q)$ at $q = 0.5 \text{ \AA}^{-1}$.

Figure 5 compares the molecular scattering functions calculated by using the six-state model for i-PMMA (solid

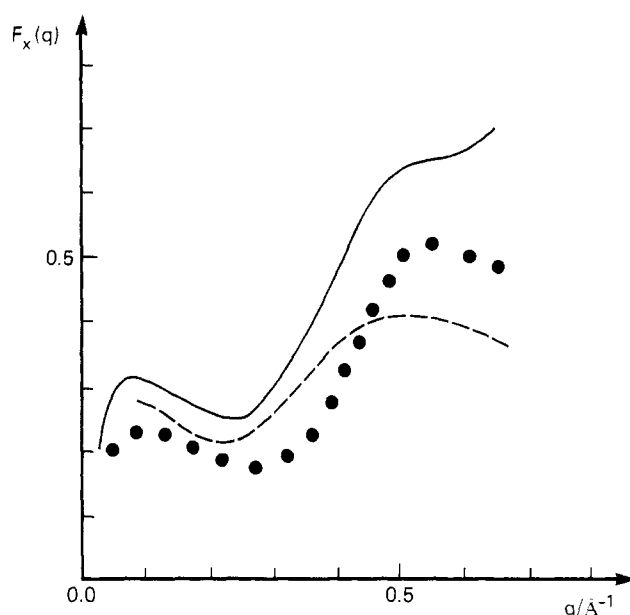


Figure 6. The molecular scattering function $F_x(q)$ of s-PMMA obtained from X-ray scattering experiments of a dilute benzene solution in ref 22 (circles) in comparison with the theoretical curves calculated according to the six-state model with the scattering centers located on C^α (solid line) and at the center of mass of the ester group (dashed line), respectively.

line) and for polymer chains containing 10% of meso diads (dot-dashed line), respectively, with the experimental results of ref 8.²⁰ The scattering curve calculated for stereochemically pure s-PMMA, not shown here, is very close to the dot-dashed curve, with only a slight increase in absolute intensity around the first maximum. The experimental results of s-PMMA (triangles) are well matched by the calculated curve, with the differences well within the fluctuations between the different experimental results of a-PMMA in Figure 3. The calculated curve for i-PMMA is similar to that predicted by the two-state model (shown in ref 11) and compares very well with experiments (circles).

Comparison with X-ray Scattering Experiments

Kirste²² determined the molecular scattering functions of s-PMMA in solutions by X-ray scattering experiments. The intensities of X-ray scattering arise from the difference in electron density between the polymer segments and solvent molecules. Hence, the loci of scattering centers are likely to be close to the C^α or the ester groups. For this reason, the molecular scattering functions determined by X-ray scattering are significantly different from those obtained by neutron scattering and thus provide further test of the six-state RIS model.

Figure 6 shows two calculated curves of $F_x(q)$ using the frame of the six-state model with the scattering centers placed on the backbone C^α atoms (solid line) and at the centers of mass of the ester groups (dashed line), respectively, in comparison with the X-ray scattering results of Kirste²² from dilute solutions of s-PMMA in benzene (filled circles). The calculated intensities are seen to be quite sensitive to the choice of the scattering centers along the chain. In reality, the X-ray scattering functions will be a weighted average of the two curves. The weighting factor is not known accurately, however. Also, benzene is not a Θ solvent for PMMA and thus its spatial configuration is likely to be modified somewhat with respect to the unperturbed state. Despite these uncertainties, the overall trend of the X-ray scattering experiment is repro-

duced quite well by the model calculations, with the intensities and the positions of all the maxima and minima in good agreement with experimental results.

Conclusions

We have compared the molecular scattering functions calculated for PMMA chains of varying stereoregularity according to the three models of the conformational statistics of this polymer proposed by Sundararajan and Flory,¹³ by Sundararajan,¹⁷ and by Vacatello and Flory.¹⁸ The scattering curves calculated for i-PMMA are virtually indistinguishable and are in very good agreement with the experimental results of O'Reilly et al.,⁸ showing that the calculated curve is not very sensitive to the details of the conformational model. The scattering functions calculated for a-PMMA are quite different, however, depending on the chain model. In all the cases a maximum is predicted in the absolute-scale Kratky plot in the region of the scattering vector q between 0.05 and 0.10 \AA^{-1} with the absolute intensity of the maximum not too different from that obtained by neutron scattering from mixtures of deuterated and normal (protonated) a-PMMA. However, the three calculated curves are markedly different at $q > 0.10 \text{\AA}^{-1}$. In particular, the two-state and the three-state models predict the occurrence of a second maximum at values of q which are considerably smaller than the experimental results of Dettenmaier et al.⁹ In contrast, the scattering function calculated in the framework of the six-state model shows the two maxima and the intervening minimum in the same locations of q as those in the experimental curve. Taking into account the extreme sensitivity of the calculated molecular scattering functions to the details of the conformational model (well evidenced by the large differences in the position of the maxima and minima of the calculated curves in Figure 4), one is led to conclude that the six-state model constitutes a fairly accurate description of the conformational statistics of PMMA not only in the over-all chain dimensions but also on a very local scale of two to three monomer units.

Of course, a RIS model with six conformational states is less manageable than the simpler two- and three-state models. The complication is only apparent, however, since the location of the states in the three-state model varies with that of the adjacent bond in the same diad. It should be recalled, on the other hand, that PMMA is an intrinsically complicated polymer. Not only the two side groups at the disubstituted C^α atom are different, but also one of them (the ester group) is devoid of cylindrical symmetry. Furthermore, the two substituents are bulky enough to cause large repulsive interactions with neighboring groups in all the chain conformations with reasonable values of the bond lengths and bond angles. For comparison, a four-state model has been recently proposed for poly(isobutylene),²³ which has two identical and cylindrically symmetric side groups. Hence, the fact that six states are necessary to describe the conformational properties of PMMA is not unreasonable.

The very good description of the experimental results of the molecular scattering function for a-PMMA up to $q \approx 0.6 \text{\AA}^{-1}$ by the six-state model deserves further comments. First of all, the basic assumptions of the RIS scheme are not applicable to PMMA a priori. That is, the conformational energy calculations of ref 18 show in fact that the energy and the exact location of the torsional states of a given diad or interdiad conformation depend on the state of the two adjacent diad segments. This dependence is weak enough, however, to permit the use of a RIS scheme in which the statistical weight param-

eters for a given two-bond sequence are averaged over all the possible low energy conformations of the two adjacent segments. Furthermore, all the conformational energy calculations have been performed up to now for pure isotactic and syndiotactic chains, while a-PMMA contains a large fraction of junctions between segments of the two kinds. Both the nature of the conformations permissible at the junctions and their relative energies are presently unknown. The agreement between experimental results and those calculated in the frame of the six-state model shows therefore that all the approximations implicit in the RIS model are not too far from the reality for PMMA.

Another remarkable observation is that the set of parameters and the location of the conformational states adopted in the present work were directly obtained in ref 18 from the conformational energy calculations and did not require adjustments to reproduce many conformation-dependent properties of i-PMMA and s-PMMA. The fact that the calculated scattering functions closely reproduce the experimental behaviour for all the stereoisomers of PMMA confirms that conformational energy calculations can be made reliable enough to describe the spatial distribution of units in a polymer chain, provided that a carefully selected set of potential energy functions and realistic approximations are employed. In this regard, it should be emphasized that reliable energy differences among conformers can be obtained, for very crowded polymers like PMMA, only if the backbone bond angles are allowed to relax independently in each conformation.

Lastly, one should emphasize that even in the case of a complicated looking polymer like PMMA the chain conformations in the bulk amorphous state correspond very closely to the unperturbed random coils. Local correlations among spatially adjacent segments belonging to different chains do not seem to affect the intramolecular properties to any appreciable extent. This appears to be true not only for the overall chain configurations but also for local chain segments constituted by a few units.

Acknowledgment. We thank IBM Italy for providing the IBM World Trade visiting professorship to MV. We also thank Drs. G. D. Wignall, J. O'Reilly, and M. Dettenmaier for the discussions on their experimental results.

References and Notes

- (1) IBM World Trade visiting professor. Permanent address: Dipartimento di Chimica, Università di Napoli, Via Mezzocannone 4, 80134-Napoli, Italy.
- (2) Deceased September 1985.
- (3) (a) Stein, R. S.; Hahn, C. C. *Phys. Today* **1985**, *74*. (b) Wignall, G. D. *Encyclopedia of Polymer Science and Engineering*; Wiley: New York, 1987; Vol. 10, p 112 and references therein.
- (4) Flory, P. J. *Statistical Mechanics of Chain Molecules*; Interscience: New York, 1969; pp 340-350.
- (5) Yoon, D. Y.; Flory, P. J. *Macromolecules* **1976**, *9*, 294.
- (6) Kriste, R. G.; Kruse, W. A.; Schelten, J. *J. Makromol. Chem.* **1972**, *162*, 299.
- (7) Kriste, R. G.; Kruse, W. A.; Ibel, K. *Polymer* **1975**, *16*, 120.
- (8) O'Reilly, J. M.; Teegarden, D. M.; Wignall, G. D. *Macromolecules* **1985**, *18*, 2747.
- (9) Dettenmaier, M.; Maconnachie, A.; Higgins, J. S.; Kausch, H. H.; Nguyen, T. Q. *Macromolecules* **1986**, *19*, 773.
- (10) Ito, H.; Russell, T. P.; Wignall, G. D. *Macromolecules* **1987**, *20*, 2213.
- (11) Yoon, D. Y.; Flory, P. J. *Polymer* **1975**, *16*, 645.
- (12) Yoon, D. Y.; Flory, P. J. *Macromolecules* **1976**, *9*, 299.
- (13) Sundararajan, P. R.; Flory, P. J. *J. Am. Chem. Soc.* **1974**, *96*, 5025.
- (14) McCrum, N. G.; Read, B. E.; Williams, G. *Anelastic and Dielectric Effects in Polymers*; Wiley: New York, 1967; pp 238-255.
- (15) O'Reilly, J. M.; Mosher, R. A. *Macromolecules* **1981**, *14*, 602.

- (16) O'Reilly, J. M.; Teegarden, D. M.; Mosher, R. A. *Macromolecules* **1981**, *14*, 1693.
- (17) Sundararajan, P. R. *Macromolecules* **1986**, *19*, 415.
- (18) Vacatello, M.; Flory, P. J. *Macromolecules* **1986**, *19*, 405.
- (19) Flory, P. J.; Sundararajan, P. R.; De Bolt, L. C. *J. Am. Chem. Soc.* **1974**, *96*, 5015.
- (20) The experimental results of ref 8 are replotted here by taking the data in Figure 4 of ref 8 and converting these directly to the $F_x(q)$ plots in the usual manner²¹ (taking the density ρ to be 1.22). Figure 9 of ref 8 underestimates the absolute values of $F_x(q)$ by ca. 10% in this regard.
- (21) Yoon, D. Y.; Flory, P. J. *Polym. Bull.* **1981**, *4*, 693.
- (22) Kirste, R. G. *Makromol. Chem.* **1967**, *101*, 91.
- (23) Suter, U. W.; Saiz, E.; Flory, P. J. *Macromolecules* **1983**, *16*, 1317.

Uniaxiality Induced in a Strained Poly(dimethylsiloxane) Network

P. Sotta* and B. Deloche

*Laboratoire de Physique des Solides, Université Paris-Sud, 91405 Orsay, France.
Received June 14, 1989; Revised Manuscript Received September 11, 1989*

ABSTRACT: The orientational order generated in a uniaxially strained polymer network is described and discussed. Experiments have been performed on an end-linked poly(dimethylsiloxane) network, using the deuterium nuclear magnetic resonance technique (²H NMR). We first recall that the resonance spectra observed in the absence of an external force reflect a local anisotropy of segmental motions, which may be related to the constraints associated with the presence of network junctions. When a uniaxial force is applied, a detailed analysis of the spectrum shows that the segmental motions become uniaxial around the external force direction. This experimental fact, which is inconsistent with noninteracting chain descriptions, is interpreted as new evidence for short-range orientational interactions between segments (introduced previously by Sotta et al. to account for free-chain orientation). A crude mean-field treatment including these interactions, together with the constraints associated to junctions, is proposed and compared with experiments.

1. Introduction

Much work, using several experimental techniques, has been devoted to investigating the anisotropy induced at a molecular scale by a macroscopic deformation in rubber polymer networks. Among these techniques, deuterium nuclear magnetic resonance (²H NMR) in principle gives access to the anisotropy and time scales of individual molecular motions, by use of a probe nucleus (²H) coupled solely with the orientation and motions of its host molecule. Thus ²H NMR has been used to study the orientational order induced in rubber networks under a uniaxial stress. The main properties, which so far have been experimentally demonstrated in poly(dimethylsiloxane) (PDMS) networks, are now reviewed briefly.

Deuterated probes, either conventional solvent molecules^{1,2} or free PDMS chains,³ have been dissolved in PDMS networks, wherein they undergo liquidlike translational diffusion (diffusion coefficient of the order 10⁻¹² m² s⁻¹). A uniaxial orientational order is induced in these probe molecules upon elongation of the network; in other words, their orientational diffusion becomes, weakly but permanently, anisotropic and uniaxial around the applied force direction. This property, and specifically the free-chain orientation, has been interpreted as an experimental evidence for orientational interactions between chains, cross-linked or not, at a segment scale.

²H NMR spectra obtained on network chains themselves exhibit more complex features, hitherto difficult to analyze quantitatively. Nevertheless, as the network is uniaxially stretched, these spectra likewise reveal a motional uniaxiality around the applied force direction.⁴

Moreover, the orientation degrees measured on network chains and guest free chains (diffusing in the network) are the same under similar conditions.³ This suggests that the correlations related to the orientational interactions quoted above may play a significant role in molecular dynamics, for both kinds of chains.

The purpose of this paper is to study in more detail the local uniaxiality reflected by the spectra of network chains, under uniaxial stress. Results particularly relevant in view of this scope are described in section 4, which emphasizes observations already published.⁴ The observed stress-induced uniaxiality, as well as the free-chain orientation previously stated, is inconsistent with descriptions in terms of independent chains: this major discrepancy is illustrated in section 5. The observed induced uniaxiality is interpreted, as earlier, as a cooperative effect of the segmental short-range interactions already mentioned. These, modeled in a simple mean-field way, result in a uniaxial orientational field (of order 1/*N*, where *N* is the average mesh size of the network). The motional anisotropy of a segment submitted to this field, additionally to constraints due to cross-link junctions, is computed; a qualitative description of ²H NMR spectra is then proposed (section 6). However, the important discrepancies that remain between experimental results and modeling are discussed (section 7). These do not question the specificity of the ²H NMR technique, which appears clearly when comparison is drawn with various optical techniques widely used in this area (section 7): these basically give access to ensemble averages of molecular orientation functions rather than to the distribution of these orientations, as is the case in ²H NMR.